JOURNAL OF MATERIALS SCIENCE 14 (1979) 2500–2508

Observations of cellular transformation products in nickel-base superalloys

CLAIRE Y. BARLOW, BRIAN RALPH
Department of Metallurgy and Materials Science, University of Cambridge, UK

Transmission electron microscopy has been used to identify the products in cellularly transformed regions of alloys based on the Nimonic 80 A composition. The commercial alloy is shown to undergo a small degree of cellular transformation even after conventional heat treatments, while recrystallization is found to increase the incidence of this reaction type. Low carbon versions of this alloy demonstrate cellular precipitation over a wider range of heat treatments.

It is shown that the cellular reaction may take place in these alloys under a variety of different conditions and with a range of driving forces. Reasons for this unexpected behaviour are offered, as is a suggestion as to why the cellular reaction occurs on a local scale.

1. Introduction

Cellular precipitation is a form of discontinuous reaction, involving grain boundary migration. Its essential features are the utilization of the moving incoherent interface as a high diffusivity reaction front, and the formation of a lamellar or rod-like aggregate behind the interface. The aggregate may contain two or more phases, and in general the interphase interfaces are of low energy, being semi-coherent or coherent [1].

The starting material for the precipitation reaction is, in the simplest case [2], a supersaturated solid solution α'. The passage of the reaction interface allows the formation of a precipitated phase, β, with an associated reduction in α supersaturation. This will be referred to as a type 1 reaction. The reaction may also begin in material containing a dispersion of β in α (type 2) [3], and here the driving force is the reduction in interphase interfacial area by replacement of the discrete precipitates with lamellae or rods of the same material. The reduction in energy in this case is less than in the solid solution instance. The third general type of reaction occurs in material already containing a metastable dispersed phase, γ [4]. This transforms to the thermodynamically more stable β phase with the passage of the reaction interface, by the reaction $\alpha+\gamma\rightarrow\alpha+\beta$. This reaction was not observed in the alloys studied here.

The effect of the presence of matrix strain, resulting from prior cold work, is in all cases to encourage the reaction [5]. This results in a lower temperature for the initiation of any of the processes, as the reduction in matrix strain energy is merely an additive term to the phase transformation energy term. The recrystallization reaction, where no phase changes are necessary, and all the migration energy derives from a reduction in matrix strain energy, is closely related to the discontinuous precipitation reaction.

Cellular precipitates normally nucleate and grow on grain boundaries, with a preference for high angle grain boundaries well away from coincidence orientations [3]. This observation is readily explained if the growth rate is determined by the rate of diffusion of solute species within the moving interface [6]. The near perfect structure of coincidence site boundaries and boundaries close to coincidence orientations precludes their use as high diffusivity paths. The more disordered structure of a high angle boundary well away from coincidence enables both diffusivity of species within the boundary and mobility of the boundary to be high [7].

The growth of cellular colonies requires the formation of nuclei of a second phase on the grain

0022–2461/79/102500–09 $02.90/0

boundary, followed by migration of the grain boundary. There is some controversy over the mechanism of the original nucleation. The two main theories are the "conventional" mechanism [8] and the "pucker" mechanism [2]. Both require the nucleation of a particle with an orientation relationship to one grain, α_1, and the subsequent movement of the grain boundary to consume the other grain, with particle growth occurring through solute diffusion along the interface. However, the driving forces differ, giving small geometrical variations. In the conventional case, the formation of a solute depleted zone behind the moving interface causes the boundary to bow outwards into the solute-rich region in grain α_2, leading to continued migration. By contrast, the "pucker" mechanism invokes a bending of the grain boundary surface by the formation of the original second phase particle, and boundary migration occurs to remove the high energy incoherent precipitate–matrix interface. The "pucker" mechanism was developed specifically for the lead–tin system by Tu and Turnbull [2], and the implication (both from the literature and from this study) is that a mechanism closer to the "conventional" mechanism is more likely in systems where the surface energy anisotropies of the precipitating phases are low.

The lamellar spacing varies between different boundaries, but is constant for colonies on any particular boundary. It is determined by the diffusion criteria and by the temperature. The precipitation, being interface controlled, occurs very much more rapidly than the equivalent volume controlled intragranular precipitation. The cellular colonies are often fan shaped [9] and the lamellar spacing is maintained through either lamellar branching [8] or through renucleation [10].

In superalloys the cellular precipitate is deleterious to mechanical properties, in particular to ductility [11, 12], and commercial treatments aim to preclude its formation. It has been postulated that the value of the γ/γ' interfacial energy is critical in determining the susceptibility of an alloy to cellular precipitation [13].

The present investigation arose as part of a study of the influence of thermomechanical treatment on the microstructure of grain boundary regions in alloys based on the Nimonic 80 A composition. Three alloys were studied: the commercial alloy, and two alloys with a lower carbon content, and cellular precipitation was found in all. The conditions under which the precipitates formed varied between the alloys; while the commercial alloy was resistant to precipitate formation, it occurred more easily in the low carbon alloys. The reduction in carbon content of these alloys resulted in a decrease in the amount of precipitation of chromium carbide ($M_{23}C_6$) at the grain boundaries. This precipitation thus reduces the overall concentration of chromium in the matrix, but more particularly, causes the formation of a region depleted in chromium adjacent to the grain boundaries [14]. Thus a reduction in the amount of chromium carbide precipitation reduces this depletion. In consequence, the local element concentrations adjacent to the grain boundaries are likely to be different in the commercial and low carbon versions of the same alloy. Chromium segregates to the matrix, γ, in preference to the dispersed γ' phase [15]. As the matrix lattice parameter is sensitive to solute concentration, this will cause a change in the γ'/γ and $M_{23}C_6/\gamma$ relative lattice parameters, and hence in their interfacial energies [15]. The experimental evidence does not therefore contradict the interfacial energy stability criterion [13]. The addition to the low carbon alloy of niobium, a strong carbide former, also had a profound effect on the microstructures generated.

2. Experimental

Material has been examined by transmission electron microscopy using a range of microscopes. Most of the work was performed with a JEM 200A microscope operating at 200 kV, but the increased resolution of a JEM 120CX operating at 100 kV has been used for the detailed investigation of some interfaces. Thicker specimen sections, more closely approximating to bulk material, were examined in an EM7 at 1 MV. The compositions of the alloys investigated are given in Table I. The heat treatments given are mainly based on two standard commercial heat treatments, with air cooling between all stages:

(1) Standard 2 stage: 2 h at 1050° C/16 h at 700° C

(2) Standard 3 stage: 2 h at 1050° C/24 h at 850° C/16 h at 700° C.

Recrystallization of the commercial alloy was performed on the two-stage heat treated material by introducing ~16% deformation by cold rolling, and holding for a range of times at temperatures between 940 and 1000° C.

TABLE I Alloy compositions (wt%)

Alloys	C	Cr	Ti	Al	Nb
Alloy 1: Commercial Nimonic 80 A	0.06	19.5	2.5	1.3	–
Alloy 2: Low carbon 80 A	0.006	19.5	2.5	1.4	–
Alloy 3: Low carbon and niobium enriched 80 A	0.006	19.5	1.3	1.7	2.0

3. Results

Cellular precipitation was seen in all three alloys, and the appearance of the colonies were similar. Laths of precipitated phase, interspersed with matrix γ were seen. The laths were for the most part normal to the grain boundary, and colonies were frequently seen extending into the grains on either side of the interface. The laths were irregular in cross-section, and showed extensive bending. The colonies in alloys 1 and 2 contained both γ' and carbide, and the morphologies and distribution of the phases were dependent on the temperature of formation. The width of the colonies was rarely more than 1 μm, but there was immense variation in the proportion of the total length of grain boundary bearing such precipitates.

3.1. Alloy 1 (commercial alloy)

Discontinuous precipitation occurred to a greater or lesser extent in most of the microstructural states of this alloy. The standard heat treatments produced predominantly discrete particles of γ' within the matrix, and "blocky" $M_{23}C_6$ particles on the grain boundaries. However, small cellular colonies were found in both standard heat treated states. Fig. 1 shows such a colony, containing all three phases normally present in the alloy: γ, γ' and carbide.

During recrystallization partial dissolution of carbide particles occurred, and when the temperature was at or above the γ' solvus the recrystallized material was supersaturated with both γ' and carbide-forming elements. These were precipitated initially by a cellular reaction on ageing at lower temperatures, as in Fig. 2. The colonies were again three-phase. If the recrystallization temperature was below the γ' solvus, colonies formed behind the recrystallization interface as in the partially recrystallized material in Fig. 3.

3.2. Alloy 2 (low carbon alloy)

The standard heat treatments both induced copious discontinuous precipitation in this alloy, as seen in Figs. 4, 5a and d. The interlamellar spacing of the colonies was dependent on the growth temperature, which together with the structure of the boundary concerned determined the diffusivity of elements along the interface. The distribution of phases within a colony is seen in the dark-field micrographs with the associated diffraction pattern in Figs. 5b, c and e. The matrix contains a dispersion of γ', and Fig. 5e demonstrates that the orientation of the γ' within the colony was close to that within the grain from which the colony grew. This is the anticipated result, and is in accordance with evidence produced by previous workers [16]. The diffraction pattern (Fig. 5b) indicates that both the γ' and carbide are in a cube–cube orientation relationship with the γ matrix.

Cellular colonies may nucleate with an orientation relationship to either grain, and their sub-

Figure 1 Alloy 1, standard 3-stage heat treatment. This shows two small cellular colonies on a grain boundary (arrowed), with one colony nucleated on each grain. In the lower colony, nucleated on the left-hand grain, laths of γ' (a, b) which have grown on a prior γ' particle (c) are indicated. The carbide laths are in dark contrast.

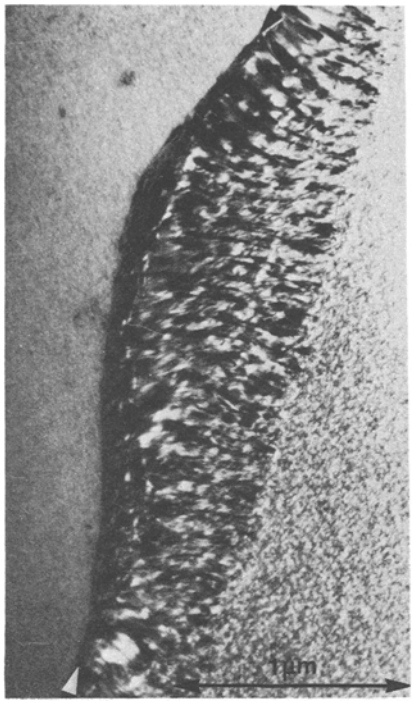

Figure 2 Alloy 1, fully recrystallized by holding for 2 min at 980° C, and subsequently aged for 18 h at 700° C. The laths within the colony are seen to be curved. The matrix contains a fine dispersion of γ', seen as a mottled background. Comparison with specimens aged for shorter times at the same temperature indicated that the growth rate of the cellular colonies decreased with time. This is in accordance with the theory that the driving force for growth decreases as the intragranular γ' increases in size.

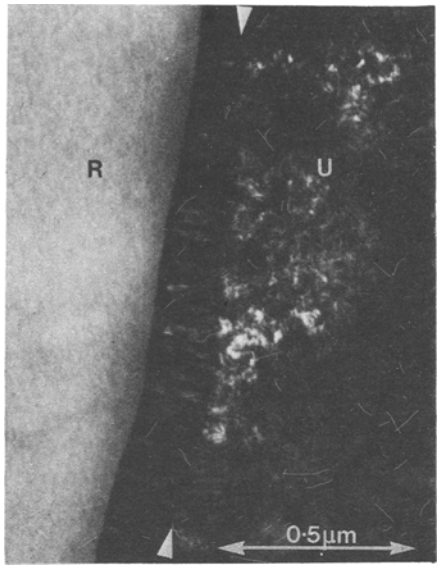

Figure 3 Alloy 1, partially recrystallized (R) by holding for 6 min at 950° C, and subsequently held for 4 h at 750° C. The effect of the second part of the heat treatment was to nucleate cellular colonies on the recrystallization interfaces already present. These grew into unrecrystallized material (U) at a constant but low rate. The recrystallization interface has thus become the reaction interface for the cellular precipitate, and moved to the indicated position.

sequent growth normal to the boundary plane gave the characteristically "wavy" appearance seen in Fig. 5d. The nucleation of the discontinuous precipitate is shown by Fig. 6 to be by the conventional mechanism, commencing with the formation of carbide particles.

3.3. Alloy 3 (low carbon niobium enriched alloy)

The cellular colonies in this material differed from all those in the other two alloys in that they contained only two phases, γ and γ', distributed in laths. Some carbide was present in the grain boundary regions, however, and can be seen in the typical colonies shown in Figs. 7a to c. The carbide is in the form of extensive sheets along the grain boundaries, coupled with some "blocky" particles. The carbide was found to be orientation related to the growing grain, and hence also to the cellular colonies. The presence of the carbide on

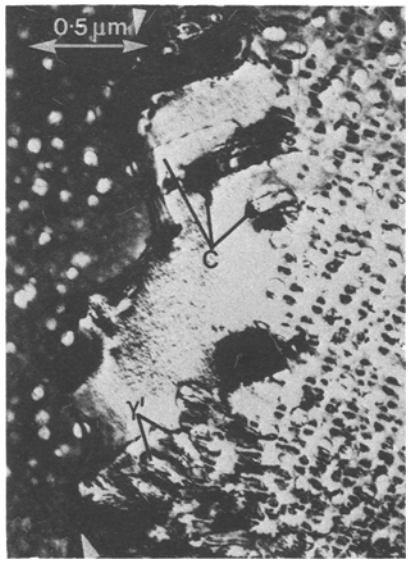

Figure 4 Alloy 2, standard three-stage heat treatment. The colony here contains rectangular plates of $M_{23}C_6$ (C) in the upper part of the micrograph, and curved rods of γ' (indicated) in the lower part. Between these two regions is an area of γ, which contains some dispersed γ' as seen from the faint mottled contrast.

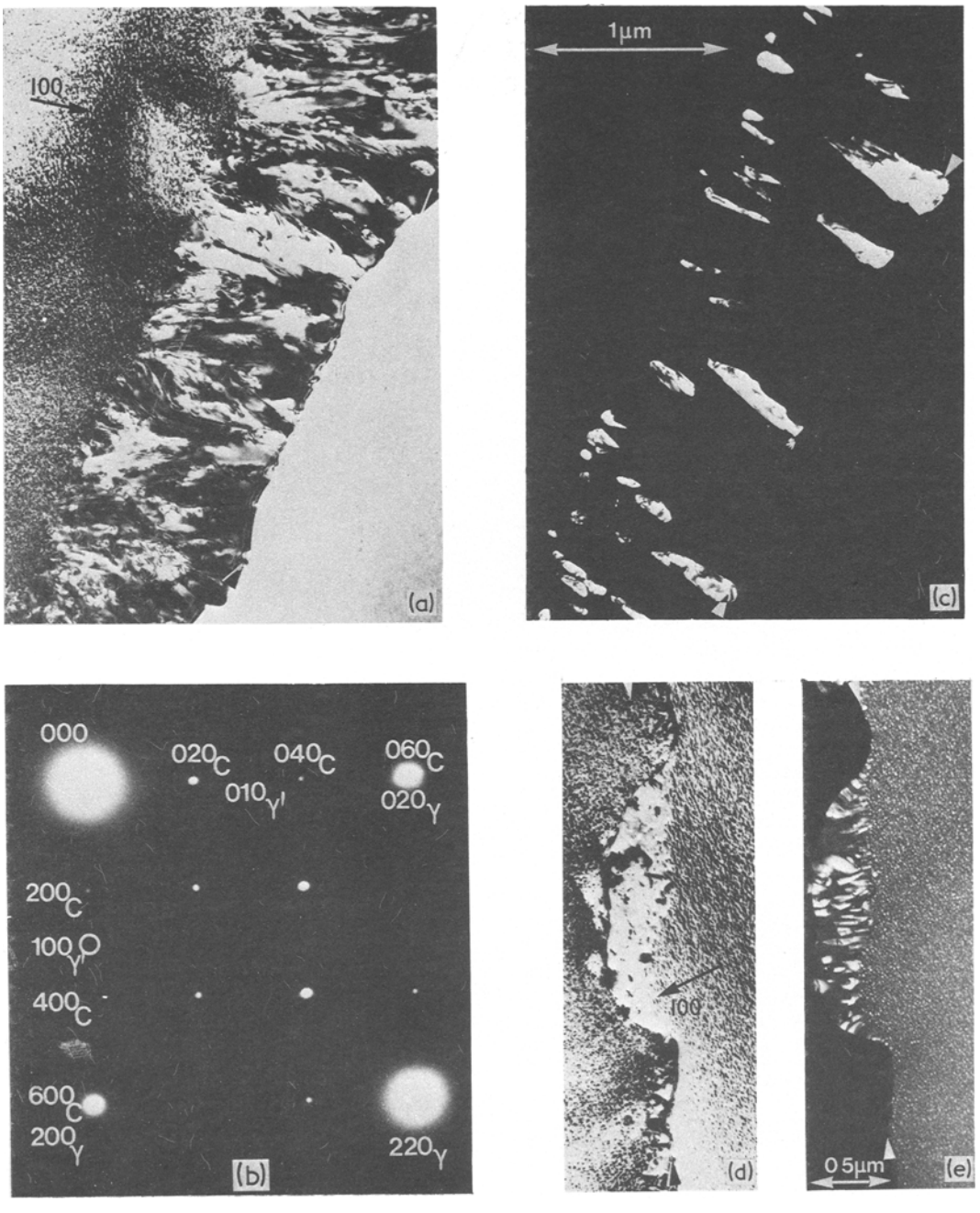

Figure 5 Alloy 2, standard two-stage heat treatment. (a) A bright-field micrograph of a well formed colony. The contrast within the colony is very complex. (b) Indexed diffraction pattern from the colony in Fig. 5a. C≡ carbide reflection (c) A dark-field micrograph (using the $1\,0\,0_C$ reflection) showing the distribution of carbide within the colony in Fig. 5a. The plates are seen to be non-uniform in thickness and irregularly spaced. The apparent discontinuity in the plates may be a result of sectioning. (d) A bright-field micrograph of a less well-developed colony than that in Fig. 5a. (e) A dark-field micrograph showing the distribution of γ' particles within the colony. The illumination of the intragranular γ' by the same reflection indicates that no significant change in orientation has occurred with the change in morphology.

Figure 6 Alloy 2, 2 h at 1050° C + 2 h at 850° C. The cellular precipitate here is all nucleated on the same grain. The boundary is slightly bowed in between the large $M_{23}C_6$ carbide particles (arrowed), and elongated γ' particles are seen. The shape of the carbide particles is typical of nuclei for cellular precipitates by the conventional mechanism.

the carbide on the grain boundaries implies that the growth of the colonies had ceased.

4. Discussion

The criteria for determining whether precipitated phases should be discrete or in cellular colonies in any instance are not clear. It is possible to categorize the principal driving force for the reaction on the basis of the types mentioned in the introduction, but there are some anomalies. The explanations seem to lie in the nucleation stages of the reaction.

4.1. Alloy 1

As a commercial alloy this is expected to be stable when containing discrete particles of both γ' and carbide, as extensive cellular precipitation leads to a reduction in ductility. Small cellular colonies are unlikely to affect mechanical properties, and are not indicative of incipient general instability. The scale of the colony in Fig. 1 indicates that it formed during the higher temperature ageing treatment, probably as a result of a local composition fluctuation due to the proximity of the large carbide particles.

The second precipitation stage in the ageing treatment (18 h at 700° C) is unlikely to have significantly affected the colony. At the start of this treatment, the matrix contains approximately 150° C supersaturation of γ' and carbide-forming elements. This would be a sufficient driving force for the growth of a cellular colony, and it would be feasible for a colony to re-nucleate at a smaller spacing, consistent with the lower temperature, and to continue to grow. However, the matrix contains large γ' particles, and for growth of the colony it would be necessary for these to be consumed, and reprecipitated in the form of fine laths. The total γ–γ' interphase interfacial area would be increased by this process, so the positive driving force of the reduction in matrix supersaturation must be outweighed by the negative effect due to interfacial energy considerations. The matrix supersaturation drops during the 700° C ageing treatment as fine γ' particles nucleate between the large particles.

The formation of cellular precipitates during ageing following recrystallization, and during low activation energy recrystallization are examples of type 1 and deformation-induced type 2 reactions respectively. However, the supersaturation at the ageing temperature of the material in Fig. 2 is considerably lower than that in the standard two-stage heat treatment, and yet the latter produces very limited amounts of cellular precipitate. This demonstrates that the criterion for the formation of cellular precipitates is not merely the degree of

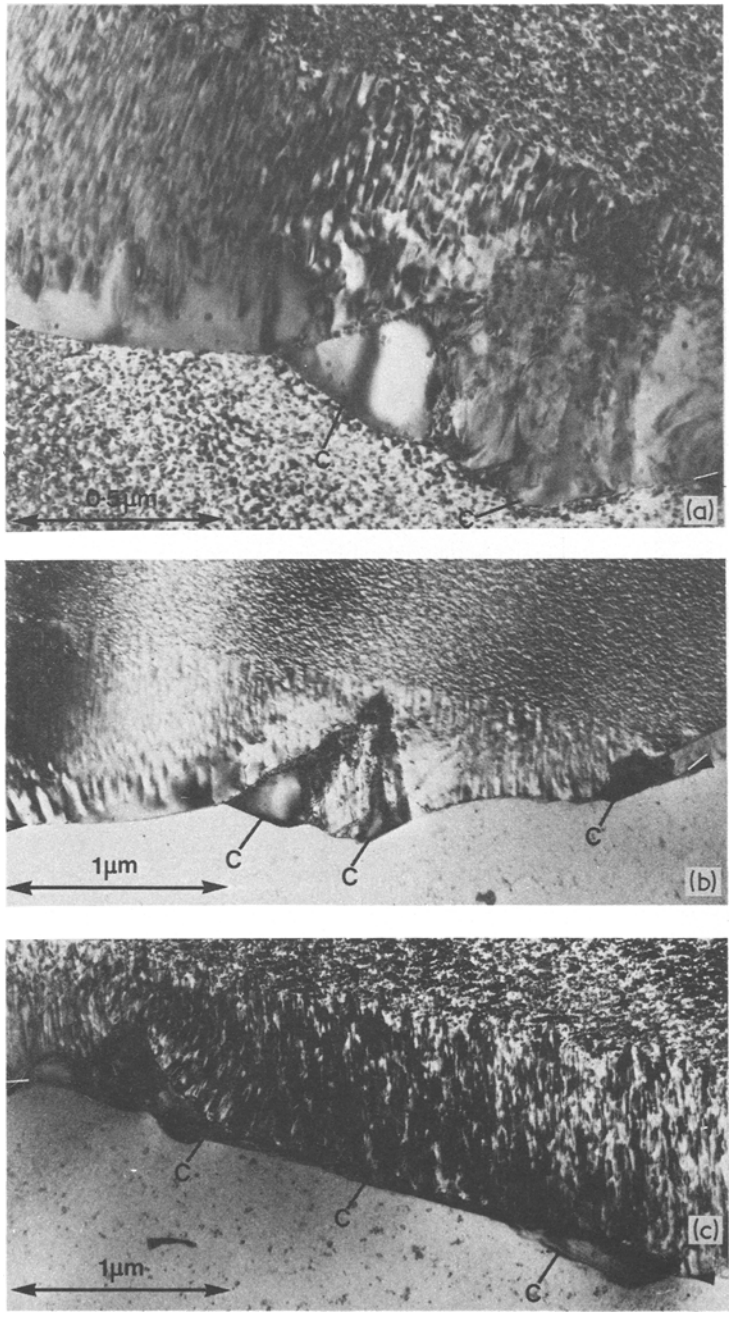

Figure 7 Alloy 3, standard two-stage heat treatment. The lamellar part of the colonies shown here contains only γ and γ', and carbide is seen at the incoherent reaction interface. (a) A perturbation in the lamellar aggregate is seen around the "blocky" carbide particles (indicated by C). (b) The same colony is seen here in a different contrast condition, in which the carbide particles are in dark contrast. (c) There is a continuous film of carbide along the incoherent interface of this colony (arrowed), and also some "blocky" particles.

supersaturation of the matrix with precipitate-forming elements.

In all cases, the first evidence of discontinuous precipitation seen in this alloy is the formation of very thin plates of $M_{23}C_6$ normal to the grain boundary plane. The plates thicken and elongate, but it is only when the colony is large enough for bowing to be evident that γ' is first seen. It is possible that discontinuous precipitation is hindered in the standard heat treatments as a result of carbide particles formed at 1050° C pinning the grain boundaries.

4.2. Alloy 2

The propensity of this alloy to cellular precipitation probably derives partly from an imbalance in the lattice parameters of the three phases [15], and hence an increase in interphase interfacial

energies. This will cause an increase in the driving force for type 2 reactions. The implication is that the grain boundary migration is less inhibited here than in alloy 1.

The distributions of γ' and carbide are notably more dissimilar and irregular in the colonies formed at high temperature. In Fig. 4, the carbide appears to be in the form of thin rectangular plates, and is well separated from the more rod-like γ'. The two phases are morphologically similar in the lower temperature form (Fig. 5a), and the spacing is more even. In Fig. 6 the spacings of the particles of both phases are reasonably constant, but very dissimilar. The spacings are approximately in proportion with the sizes of the particles.

These observations are in accordance with the following explanation. At higher temperatures the driving force for cellular precipitation is reduced, while the diffusivity along the moving grain boundary is still large [17]. The particles will thus display a greater degree of preferred morphology. At lower temperatures more constraint on morphology is imposed by the high cooperative growth rate of the colony. The comparatively small size of the γ' particles may derive from the size limit for maintenance of a coherent interphase interface.

4.3. Alloy 3

The nucleation sequence here is rather different from that in the two previous alloys. The first phase to form is γ', and carbide has precipitated at a later stage, when the solute rejection ahead of the interface has generated a sufficiently high supersaturation. The morphology of the carbide is expected to hinder, or in extreme cases halt the growth of the colony (e.g. as in Fig. 7c). Some mechanical evidence on a similar alloy also indicates that cellular precipitation is hindered [18]. The lattice mismatch between niobium carbide and the matrix is about 25%, and this is likely to cause a high nucleation energy for the phase. It is thus expected to grow in situations where there is a disordered, open structure with a high supersaturation of vacancies, such as at a moving interface [17]. Niobium would have been rejected by the growing colony, causing a build-up of concentration in the region of the moving interface. Carbide nucleation occurred when both vacancy concentration and the supersaturation of carbide-forming elements were sufficient.

5. Conclusion

Despite the wide range of heat treatments applied to the alloys studied, it was rare to find a specimen which did not contain some cellular precipitate. This result was unexpected, and raised the question of why cellular precipitates formed preferentially to discrete precipitates under some circumstances. The "local" formation of cellular colonies in standard heat treated states of the commercial alloy were particularly difficult to justify. It would seem that Nimonic 80 A is close to being unstable with respect to cellular precipitation. Thus any deviations from the established "standard" heat treatment sequences, or small changes in alloy composition, are likely to increase the extent of cellular precipitates.

The nucleation of cellular colonies in alloys 1 and 2 seemed to require the formation of suitable carbide particles on the grain boundary. These then elongated normal to the boundary using the incoherent interface for growth, causing grain boundary migration. The colonies thus appeared to nucleate by the conventional mechanism. γ' then nucleated between the carbide laths, and the two phases precipitated simultaneously with the growth of the colony. By contrast, in alloy 3 the role of the carbide, appearing as it did on the mobile reaction interface, was to hinder the growth of the cell rather than to initiate it.

Nucleation of cellular precipitates requires both diffusion along and migration of a grain boundary. In cases where the driving force for nucleation is small, as in the isolated colonies in Fig. 1, the boundaries or sections of boundary in which these processes occur most readily will be the favoured sites for nucleation. A quality of the boundary likely to be significant in this context is its local "open-ness" [7]. An open structure will facilitate both diffusion and boundary migration, and is hence advantageous for nucleation of cellular colonies. Such open structures could be achieved locally by discontinuities in the periodic structure of a grain boundary, caused by changes in grain boundary planes or misorientations.

Acknowledgements

The authors are grateful to Professor R. W. K. Honeycombe for the provision of laboratory facilities. Financial support (including a maintenance award for C.Y.B.) is gratefully acknowledged from the National Physical Laboratory. One of the

alloys was specially prepared by the European Research and Development Centre of Inco. Valuable discussions with Roger Ecob and John Bee are acknowledged.

References

1. H. I. AARONSON and H. B. AARON, *Met Trans.* 3 (1972) 2743.
2. K. N. TU and D. TURNBULL, *Acta Met.* 15 (1967) 369.
3. E. HORNBOGEN, *Met. Trans.* 3 (1972) 2717.
4. G. R. SPEICH, *Trans. AIME* 227 (1963) 754.
5. M. S. SULONEN, *Acta Met.* 8 (1960) 669.
6. J. W. CAHN, *ibid.* 4 (1956) 217.
7. H. GLEITER and B. CHALMERS, *Prog. in Mater. Sci.* 16 (1972) 1.
8. R. FOURNELLE and J. B. CLARK, *Met. Trans.* 3 (1972) 2757.
9. E. NES and H. BILLDAL, *Acta Met.* 25 (1977) 1039.
10. B. E. SUNDQUIST, *Met. Trans.* 4 (1973) 1919.
11. P. S. KOTVAL and H. HATWELL, *Trans. Met. Soc. AIME* 245 (1969) 1821.
12. E. L. RAYMOND, *ibid.* 239 (1967) 1415.
13. W. C. HAGEL and H. J. BEATTIE, *ibid.* 215 (1959) 967.
14. E. A. FELL, *Metallurgia* 63 (1961) 157.
15. G. P. SABOL and R. STICKLER, *Phys. Stat. Sol.* 35 (1969) 11.
16. C. S. SMITH, *Trans. ASM* 45 (1953) 533.
17. K. SMIDODA, W. GOTTSCHALK and H. GLEITER, *Acta Met* 26 (1978) 1833.
18. T. B. GIBBONS and B. E. HOPKINS, *Met. Sci. J.* 8 (1974) 203.

Received 13 and accepted 23 February 1979.